Facile Surface Functionalization of Hydrophobic Magnetic Nanoparticles

Yuan Liu,[†,§] Tao Chen,[†,‡,§] Cuichen Wu,[†] Liping Qiu,[‡] Rong Hu,[‡] Juan Li,[†] Sena Cansiz,[†] Liqin Zhang,[†] Cheng Cui,[†] Guizhi Zhu,[†,‡] Mingxu You,[†,‡] Tao Zhang,[†] and Weihong Tan[†,‡,*]

[†]Center for Research at Bio/Nano Interface, Department of Chemistry and Department of Physiology and Functional Genomics, Shands Cancer Center, UF Genetics Institute and McKnight Brain Institute, University of Florida, Gainesville, Florida 32611-7200, United States

[‡]Molecular Science and Biomedicine Laboratory, State Key Laboratory for Chemo/Bio-Sensing and Chemometrics, College of Biology, College of Chemistry and Chemical Engineering, and Collaborative Research Center of Molecular Engineering for Theranostics, Hunan University, Changsha 410082, China

Ⓢ *Supporting Information*

ABSTRACT: Nonpolar phase synthesized hydrophobic nanocrystals show attractive properties and have demonstrated prominent potential in biomedical applications. However, the preparation of biocompatible nanocrystals is made difficult by the presence of hydrophobic surfactant stabilizer on their surfaces. To address this limitation, we have developed a facile, high efficiency, single-phase and low-cost method to convert hydrophobic magnetic nanoparticles (MNPs) to an aqueous phase using tetrahydrofuran, NaOH and 3,4-dihydroxyhydrocinnamic acid without any complicated organic synthesis. The as-transferred hydrophilic MNPs are water-soluble over a wide pH range (pH = 3−12), and the solubility is pH-controllable. Furthermore, the as-transferred MNPs with carboxylate can be readily adapted with further surface functionalization, varying from small molecule dyes to oligonucleotides and enzymes. Finally, the strategy developed here can easily be extended to other types of hydrophobic nanoparticles to facilitate biomedical applications of nanomaterials.

Hydrophobic nanocrystals synthesized in nonpolar solvents by high-temperature thermolysis show attractive properties, such as tunable size with narrow size distribution, and low crystalline defect.[1,2] Among these materials, magnetic nanoparticles (MNPs), because of their unique nanoscale physical and chemical properties, have demonstrated prominent potential in biomedical applications, including magnetic resonance imaging (MRI),[3−5] targeted drug delivery,[6,7] and hyperthermia for cancer treatment.[8−11]

Despite their success in biomedical science, the preparation of biocompatible MNPs is made difficult by the presence of a hydrophobic surfactant stabilizer on their surfaces. To solve this problem, many strategies have been developed to transfer the hydrophobic MNPs into an aqueous phase. One popular method is ligand exchange, in which small molecules are used to replace the hydrophobic ligand. The other is amphiphilic ligand encapsulation, which involves formation of a hydrophilic shell on the surface of MNPs. Unfortunately, the ligand exchange method is typically performed in two phases: MNPs

in the hydrophobic phase and small molecules in the hydrophilic phase.[5,12,13] For example, dopamine hydrochloride has been used for ligand exchange on MNPs.[14−16] However, because of the lack of solubility in nonpolar solvents, a two-phase system is needed. Furthermore, MNPs tend to aggregate when mixed with polar solvents. Thus, the exchange efficiency is typically low because of inefficient interaction between the MNPs and small molecules, and further aggregation may occur from the low exchange ratio. In addition, dopamine-transferred MNPs have poor biocompatibility as a result of poor solubility in biological buffers. Although scientists have tried various modifications, such as the addition of PEG, to the small molecules to improve the stability of MNPs, extensive organic syntheses are needed, which are time-consuming and labor-intensive, thus making the ligand exchange method more complicated. Amphiphilic ligand encapsulation is simple, but it may not result in stable MNPs by the noncovalent hydrophobic interactions, and additional organic syntheses are necessary as well.

To address these obstacles, we have developed a facile, high efficiency, single-phase and low-cost method to transfer hydrophobic MNPs to an aqueous phase over a wide pH range (pH = 3−12) using 3,4-dihydroxyhydrocinnamic acid (DHCA) in tetrahydrofuran (THF). As shown in Scheme 1,

Scheme 1. Ligand Exchange Using Tetrahydrofuran, 3,4-Dihydroxyhydrocinnamic Acid (DHAC) and NaOH
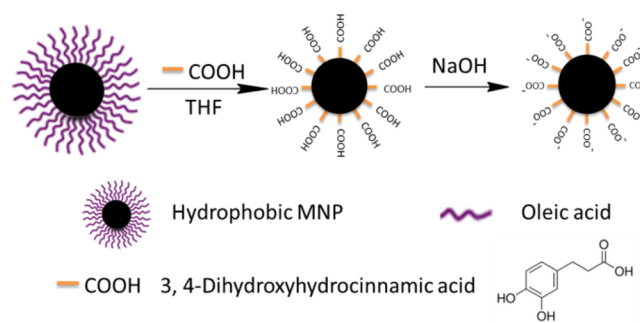
the surfactant stabilizer oleic acid was replaced by DHCA, which forms a robust anchor on the surface of magnetic nanoparticles via a five-membered metallocyclic chelate. The MNPs were then neutralized with NaOH to precipitate the sodium salt, which is not soluble in THF. The ionic form was then dispersed in aqueous solution at moderate concentrations. The resulting water-soluble MNPs were very stable over a wide pH range from 3 to 12 (Figures S4 and S5 in Support Information (SI)). In addition, MNPs coated with DHCA can be robustly functionalized via the carboxyl group to form a peptide linkage with other amine-containing molecules, varying from small molecule dyes to oligonucleotides and even enzymes. Typically, DHCA without modification was dissolved in THF in a three-necked flask. Hydrophobic MNPs (27.6 ± 1.5 nm) were added dropwise at 50 °C and kept for 3 h at this temperature. Upon cooling the reaction mixture, NaOH (0.5 M) was added to precipitate the MNPs, which were collected by centrifugation and redispersed in water. The as-transferred MNPs were spherical and fairly monodisperse without aggregation, as shown by transmission electron microscopy (TEM) images (Figure 1) and dynamic light scattering (DLS) (Figure S7, SI).
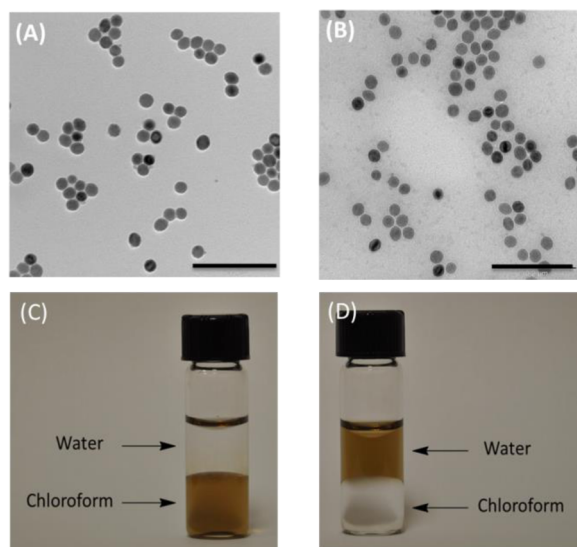

Figure 1. TEM images of magnetic nanoparticles before ligand exchange in chloroform (A) and after ligand exchange in water (B). Scale bar is 200 nm. Solvent dispersity of MNPs (C) before and (D) after ligand exchange.

After ligand exchange, water with pH values ranging from 1 to 12 was used to test the solubility and stability of the as-transferred MNPs. MNPs aggregated when the pH was 2 or lower (Figure S4, SI). When NaOH (0.5 M) was introduced to the aggregated MNPs (pH = 2) to raise the pH to 7, the aggregated MNPs dissociated and redissolved, and the soluble MNPs aggregated when HCl (0.1 M) was added to decrease the pH to 2 or lower (Figure 2). Thus, the aggregation and dispersion of MNPs is reversible by controlling the pH.

Isoelectric point precipitation (IPP) was introduced to explain the reversibility of MNP aggregation. IPP is the pH at which the net primary charges of a protein become zero, leading to aggregation because of reduced electrostatic repulsions. The IPP value for MNPs was experimentally determined to be 2 according to the solubility test above. To
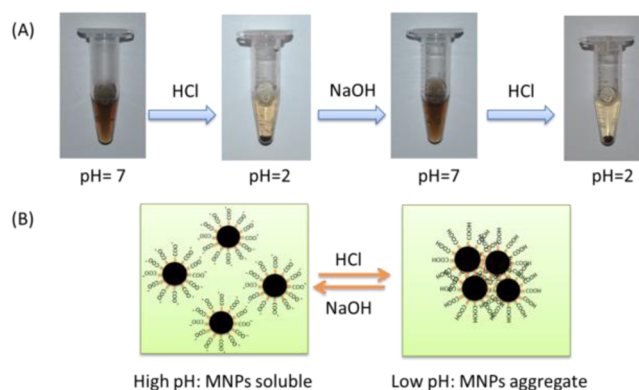

Figure 2. (A) pH-dependent solubility of MNPs and (B) schematic illustration of pH controlled reversible aggregation and dissociation of MNPs.

prove this hypothesis, the zeta-potentials of as-transferred MNPs at different pH values were measured (Figure S6, SI). Consistent with the solubility test, the results showed that the zeta-potential of an MNP is −1.4 mV at pH 2. Addition of NaOH makes the MNP surfaces more negative, thus increasing the electrostatic repulsion between the MNPs and allowing them to be dispersed in water (Figure 2B). Both TEM images and DLS results in water with different pH values indicate that the MNPs were monodisperse and stable for a period of several months. In addition, to test the stability of as-transferred MNPs, either phosphate buffered saline (PBS) or cell culture medium was used as solvent and no obvious aggregation was observed over a period of 3 months.

DHCA anions not only offer MNPs excellent water solubility but also provide a platform for further surface functionalization via the carboxyl group to form a peptide linkage with amine-containing molecules. Therefore, we systematically investigated surface functionalization with fluoresceinamine (FLAM), a DNA aptamer, and an enzyme. FLAM was chosen as a model small-molecule probe to test MNP surface functionalization because FLAM has an amine group which can form a peptide bond with the carboxyl group by 1-ethyl-3-(3-(dimethylamino)ropyl)arbodiimide hydrochloride (EDC)/N-hydroxysuccinimide (NHS) coupling to give emission at 519 nm. To rule out the possibility of physical adsorption, a control experiment was conducted with and without EDC/NHS coupling. Fluorescence measurements (Figure S8, SI) showed that MNP and MNP/FLAM without EDC/NHS coupling do not fluoresce, while MNP/FLAM with the EDC/NHS cross-linking gives a significant fluorescent signal at 519 nm, indicating that FLAM was covalently linked onto the surface of MNPs, and that the carboxylated MNP surface could serve as a platform for robust biomolecule functionalization.

Having determined that the as-transferred MNPs are stable in biological systems, we next established their utility in biomedical applications. Amine-modified Sgc8 aptamer (ASAT) (see Table S1 for all DNA sequences[17]) labeled with carboxytetramethylrhodamine (TAMRA) was used to modify MNPs based on EDC/NHS coupling and to test their binding ability to target cancer cells. In this study, we designed an amine-modified random oligonucleotide library labeled with TAMRA (ALT) as control to ASAT (Table S1, SI). Selected from a large library by SELEX (Systematic Evolution of Ligands by Exponential Enrichment), aptamers are single-stranded oligonucleotides, which specifically bind to their targets

(CEM cells for Sgc8) by folding into distinct secondary or tertiary structures.[18] Ramos cells, which are not recognized by Sgc8, were chosen as control cells. According to the flow cytometry histogram (Figure 3), a large shift was observed for
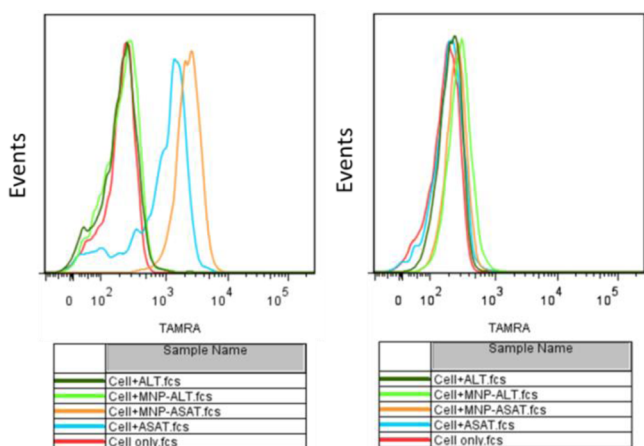

Figure 3. Flow cytometry histograms of CEM (target) and Ramos (control) cells incubated with buffer only, ASAT, MNP-ASAT, MNP-ALT, and ALT. The concentrations for all probes are 1 nM.

CEM cells, while only a negligible shift was observed for Ramos cells when treated with MNP-ASAT. For MNP-ALT, no obvious shift was observed for either CEM or Ramos cells. For target CEM cells, a slightly larger shift was observed for MNP-ASAT compared to free ASAT. This can be attributed to the multivalent effect of multiple aptamers on the surface of MNP-ASAT, thus resulting in enhanced binding affinity to the target cancer cells. Thus, the ASAT-modified MNPs have excellent binding ability on target cancer cells and can be used as specific fluorescence imaging agents.

Protein enzymes, while being widely used because of their high biocatalytic activity, are limited by their low stability and low recycling capability. Nanobiocatalysis, whereby an enzyme is immobilized on a nanoparticle surface while retaining its biocatalytic activity, is of significant importance for industrial reuse.[19,20] Therefore, we conducted a facile and robust covalent enzyme immobilization on the MNP surface using alkaline phosphatase (AP) as a model enzyme (Scheme 2). The

Scheme 2. Covalent MNP Surface Functionalization with Alkaline Phosphatase
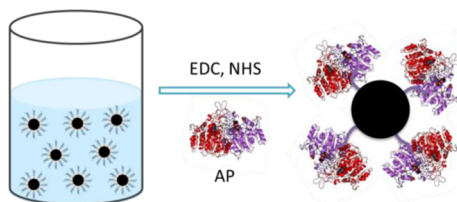
hydrolysis of *p*-nitrophenyl phosphate can be catalyzed efficiently by AP when pH = 9.8. The assay results (Figure S2, SI) indicated that MNP-AP possesses excellent catalytic activity. A 10-round catalytic recycle of MNP-AP demonstrated that MNP-AP retains its catalytic activity after many uses, indicating that the as-transferred MNP is an excellent nanosupporter for enzyme immobilization (Figure S3, SI).

In summary, we have developed a facile, high-efficiency, single-phase and low-cost method for aqueous phase transfer of hydrophobic MNPs using DHCA and THF. Without any complicated organic synthesis, MNPs neutralized with NaOH show excellent water solubility and stability in biological environments, demonstrating that the approach is more cost-effective and labor-efficient than the traditional two-phase ligand exchange method. Moreover, we report the first hydrophilic nanoparticles with wide pH-range solubility and pH-controllable aggregation. The as-transferred MNPs with carboxylate can be readily adapted by further surface functionalization which is simple and robust. On the basis of these superior features, we believe that this method can be applied to other ligand exchange methods for nanocrystals, such as quantum dots and nanorods, and that the as-transferred nanoparticles will find widespread application in nano-biotechnology.

■ ASSOCIATED CONTENT

Ⓢ Supporting Information

Detailed synthesis and characterization of hydrophobic magnetic nanoparticles, phase transfer, surface functionalization and detailed experimental procedures. This material is available free of charge via the Internet at http://pubs.acs.org.

■ AUTHOR INFORMATION

Corresponding Author

tan@chem.ufl.edu

Author Contributions

§T.C. and Y.L. contributed equally to this work.

Notes

The authors declare no competing financial interest.

■ ACKNOWLEDGMENTS

■ REFERENCES

(1) Park, J.; An, K.; Hwang, Y.; Park, J.; Noh, H.; Kim, J.; Park, J.; Hwang, N.; Hyeon, T. *Nat. Mater.* **2004**, *3*, 891−895.

(2) Lynch, J.; Zhuang, J.; Wang, T.; LaMontagne, D.; Wu, H.; Cao, Y. C. *J. Am. Chem. Soc.* **2011**, *133*, 12664−12674.

(3) Perez, J. M.; Josephson, L.; O'Loughlin, T.; Hogemann, D.; Weissleder, T. *Nat. Biotechnol.* **2002**, *20*, 816−820.

(4) Huh, Y.; Jun, Y.; Song, H.; Kim, S.; Choi, J.; Lee, J.; Yoon, S.; Kim, K.; Shin, J.; Suh, J.; Cheon, J. *J. Am. Chem. Soc.* **2005**, *127*, 12387−12391.

(5) Chen, T.; Ocsoy, I.; Yuan, Q.; Wang, R.; You, M.; Zhao, Z.; Song, E.; Zhang, X.; Tan, W. *J. Am. Chem. Soc.* **2012**, *134*, 13164−12167. Yuan, Q.; Wu, Y.; Wang, J.; Lu, D.; Zhao, Z.; Liu, T.; Zhang, X.; Tan, W. *Angew. Chem., Int. Ed.* **2013**, *52*, 13965.

(6) Cheng, K.; Peng, S.; Xu, C.; Sun, S. *J. Am. Chem. Soc.* **2009**, *131*, 10637−10644.

(7) Chen, T.; Shukoor, M. I.; Wang, T.; Zhao, Z.; Yuan, Q.; Bamrungsap, S.; Xiong, X.; Tan, W. *ACS Nano* **2011**, *5*, 7866−7873. Zhao, Z.; Fan, H.; Zhou, G.; Bai, H.; Liang, H.; Zhang, X.; Tan, W. *J. Am. Chem. Soc.* **2014**, *136*, 11220−11223.

(8) Fortin, J.; Wilhelm, C.; Servais, J.; Menager, C.; Bacri, J.; Gazeau, F. *J. Am. Chem. Soc.* **2007**, *129*, 2628−2635.

(9) Guardia, P.; Corato, R. D.; Lartigue, L.; Wilhelm, C.; Espinosa, A.; Garcia-Hernandez, M.; Gazeau, F.; Manna, L.; Pellegrino, T. *ACS Nano* **2012**, *6*, 3080−3091.

(10) Lee, J.; Jang, J.; Choi, J.; Moon, S. H.; Noh, S.; Kim, J.; Kim, J.; Kim, I.; Park, K. I.; Cheon, J. *Nat. Nanotechnol.* **2011**, *6*, 418−422.

(11) Martinez-Boubeta, C.; Simeonidis, K.; Makridis, A.; Angelakeris, M.; Lglesias, O.; Guardia, P.; Cabot, A.; Yedra, L.; Estrade, S.; Peiro, F.; Saghi, Z.; Midgley, P. A.; Conde-Leboran, I.; Serantes, D.; Baldomir, D. *Sci. Rep.* **2013**, *3*, 1652−1659.

(12) Michalet, X.; Pinaud, F. F.; Bentolila, L. A.; Tsay, J. M.; Doose, S.; Li, J. J.; Sundaresan, G.; Wu, A. M.; Gambhir, S. S.; Weiss, S. *Science* **2005**, *307*, 538−544.

(13) Tong, S.; Hou, S.; Ren, B.; Zheng, Z.; Bao, G. *Nano Lett.* **2011**, *11*, 3720−3726.

(14) Xu, C.; Xu, K.; Gu, H.; Zheng, R.; Liu, H.; Zhang, X.; Guo, Z.; Xu, B. *J. Am. Chem. Soc.* **2004**, *126*, 9938−9939.

(15) Shultz, M. D.; Reveles, J. U.; Khanna, S. N.; Carpenter, E. E. *J. Am. Chem. Soc.* **2007**, *129*, 2482−2487.

(16) Mazur, M.; Barras, A.; Kuncser, V.; Galatanu, A.; Zaitzev, V.; Turcheniuk, K. V.; Woisel, P.; Lyskawa, J.; Laure, W.; Siriwardena, A.; Boukherroub, R.; Szunerits, S. *Nanoscale* **2013**, *5*, 2692−2702.

(17) Shangguan, D.; Li, Y.; Tang, Z.; Cao, Z. C.; Chen, H. W.; Mallikaratchy, P.; Sefah, K.; Yang, C. J.; Tan, W. *Proc. Natl. Acad. Sci. U.S.A.* **2006**, *103*, 11838−11843.

(18) Sefah, K.; Shangguan, D.; Xiong, X.; O'Donoghue, M. B.; Tan, W. *Nat. Protoc.* **2010**, *5*, 1169−1185. Hu, R.; Zhang, X.; Zhao, Z.; Zhu, G.; Chen, T.; Fu, T.; Tan, W. *Angew. Chem., Int. Ed.* **2014**, *53*, 5821−5826.

(19) Luckarift, H. R.; Spain, J. C.; Naik, R. R.; Stone, M. O. *Nat. Biotechnol.* **2004**, *22*, 211−213.

(20) Sapsford, K. E.; Algar, W. R.; Berti, L.; Gemmill, K. B.; Casey, B. J.; Oh, E.; Stewart, M. H.; Medintz, I. L. *Chem. Rev.* **2013**, *113*, 1904−2074.